

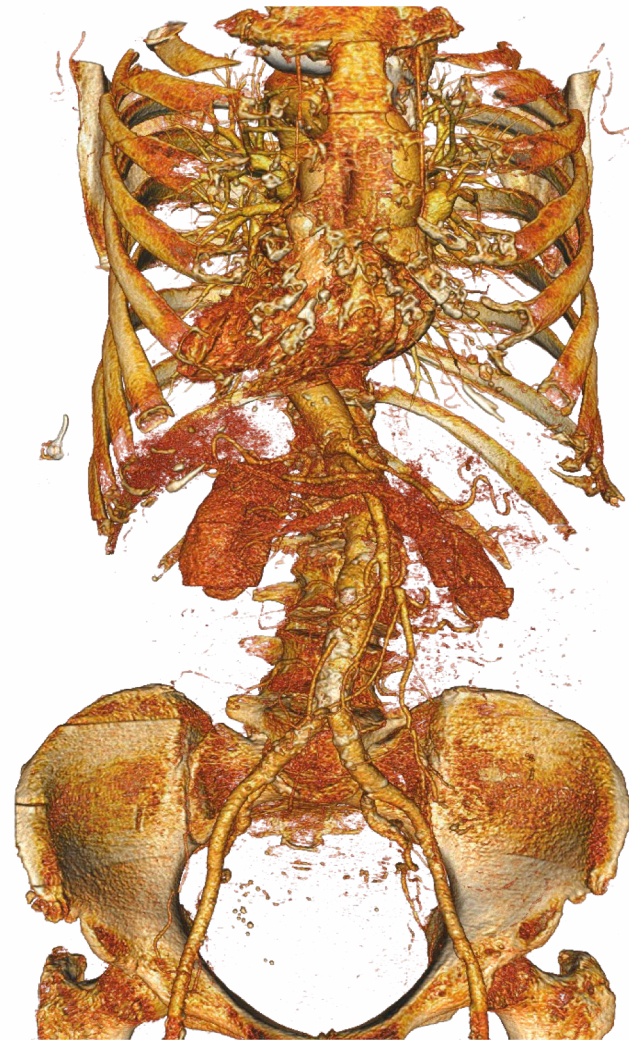
Lossless Compression for Volumetric Medical Images Using Deep Neural Network with Local Sampling

O. Nagoor, J. Whittle, J. Deng, B. Mora, M. W. Jones

Department of Computer Science, Swansea University, UK



Swansea University
Prifysgol Abertawe



Session: 3D-01 -- 3D Image and Video Analysis and Compression

Presented by: Omniah Nagoor

Introduction

- ❖ Data compression forms a central role in handling the bottleneck of data **storage, transmission and processing**.
- ❖ Data compression techniques can be divided into two main types: **lossy** and **lossless compression**.
- ❖ Choosing which type to use **relies on the application requirements**.
- ❖ For **medical** image compression, the **lossless** approach is more appropriate since it **recovers** the original data **without any loss in quality**.

Related Work

State-of-the-art **Classical Methods: (Lossless)**

- ❖ **Image Encoder:**

JPEG2000 [1], JPEG-LS [2], CALIC [3], MRP [4].

- ❖ **Volumetric Encoder:**

JP3D [5], HEVC [6], 3D-CALIC [7], M-CALIC [8], 3D-MRP [9].

Related Work

State-of-the-art Deep Learning Methods: **(Lossy)**

- ❖ Dimensionality reduction (Autoencoders) [10].
- ❖ Super-resolution images or video reconstruction [11].
- ❖ Estimating pixel likelihood (Auto-regressive) [12].
- ❖ Generative compression [13].

Related Work

State-of-the-art Deep Learning Methods: **(Lossless)**

- ❖ The current deep learning literature for lossless compression usually combine a **density estimator** model with an **arithmetic coder**.
- ❖ The **density estimator** can be categorized into various **types**:
 - Fully connected NN [14].
 - Recurrent Neural Network (LSTM/GRU) (DeepZip) [15].
 - A recursive bits-back coding with hierarchical latent variables (Bit-Swap) [16].

Motivation

- ❖ According to Diagnostic Imaging Dataset Statistical Release published by **NHS**, between September 2018 to September 2019 over **45 million medical images** acquired for clinical use including **5.8M CT scans** and **3.7M MRI scans** [17].



Motivation

- ❖ Especially for clinical purposes, **artefacts** that introduced by **lossy** compression could result in **misleading diagnosis** and **unfavorable treatment**.



Motivation

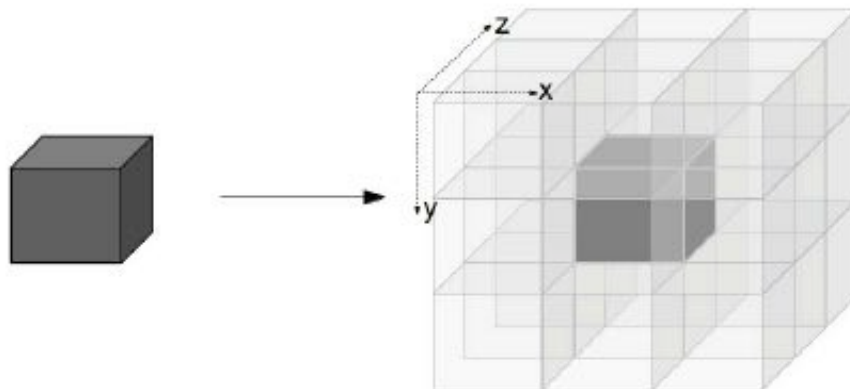
- There is a need for a compression tools that:
 - ❖ Utilizes **deep learning technique** for **Lossless** compression performance.
 - ❖ Has **computationally efficient** (parallelized) encoding/decoding performance.
 - ❖ Achieves a **higher compression ratio** compared to the state-of-the-art lossless compression methods.

Contributions

- ❖ A novel 3D predictor model using neural network that achieves **lossless compression** for **volumetric medical images**.
- ❖ A computationally efficient model that achieves **higher compression ratio** when compared to state-of-the-art lossless compression methods.
- ❖ Empirically, demonstrate the **robustness and generalization** of our proposed models on many datasets for higher dynamic range (16 bit-depths).

Proposed Method

- ❖ The **regression** problem can be solved **by** learning a mapping function f that predict the **output** \hat{y} from an **input sequence** X through the **back-propagation process** given a training dataset.

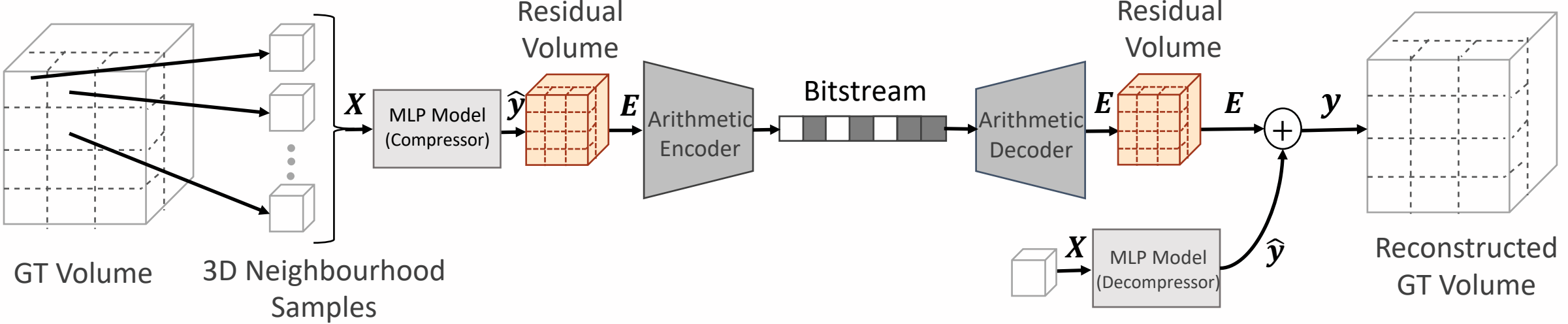


Proposed Method

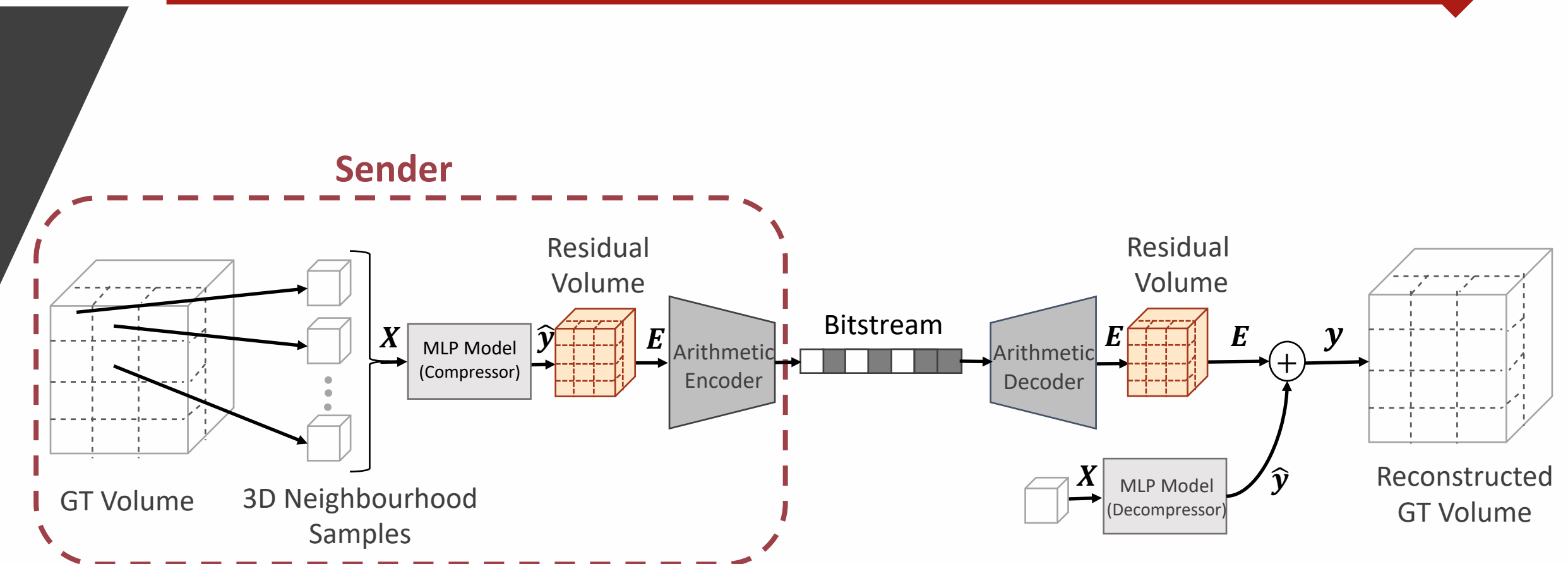
- ❖ Given a data distribution defined over $X \in R^N$, where X contains input samples from the same distribution $X = \{x_1, x_2, \dots, x_n\}$ forms a 1D vector of immediately neighboring voxel-intensities.
- ❖ We learn a **differentiable mapping function** $\hat{y} = f(X)$ that maps the **input vector X** to a **predicted value \hat{y}** to minimize the differences with the **ground truth voxel value y** , where $f(X)$ is represented using a neural network model.
- ❖ The residual (prediction) error E :

$$E = y - \hat{y}$$

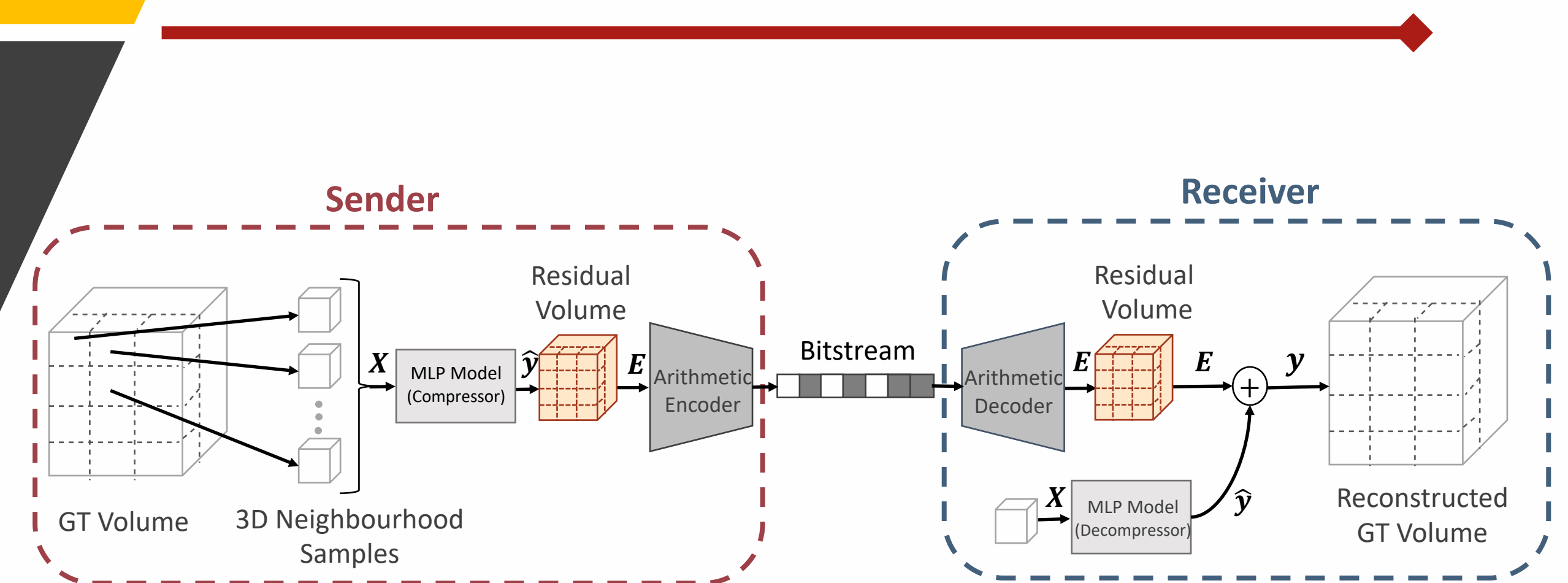
Proposed Method



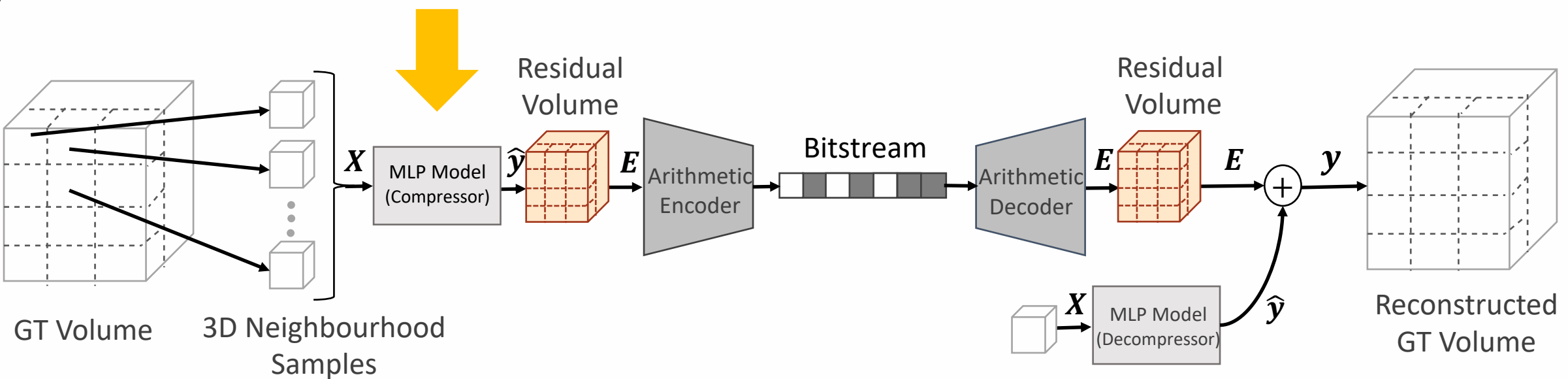
Proposed Method



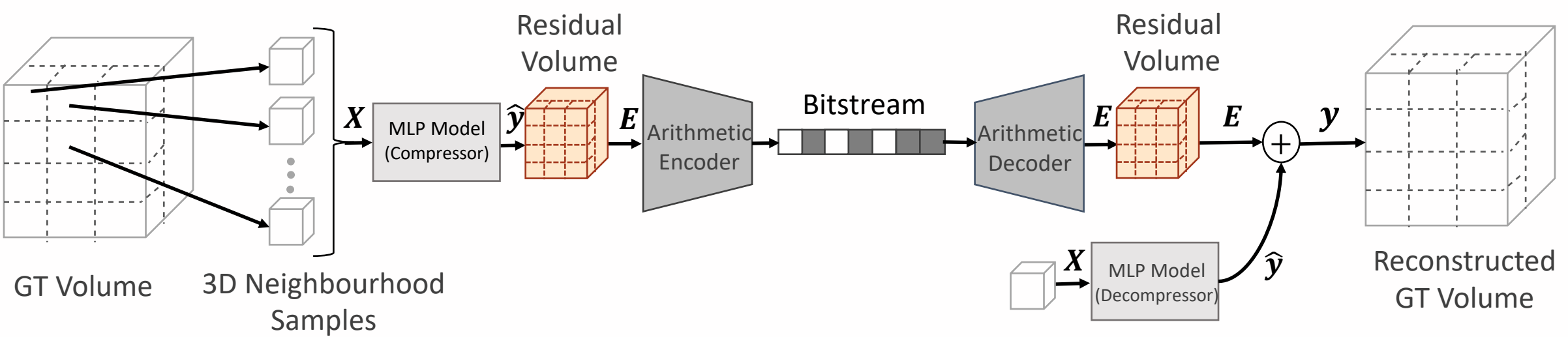
Proposed Method



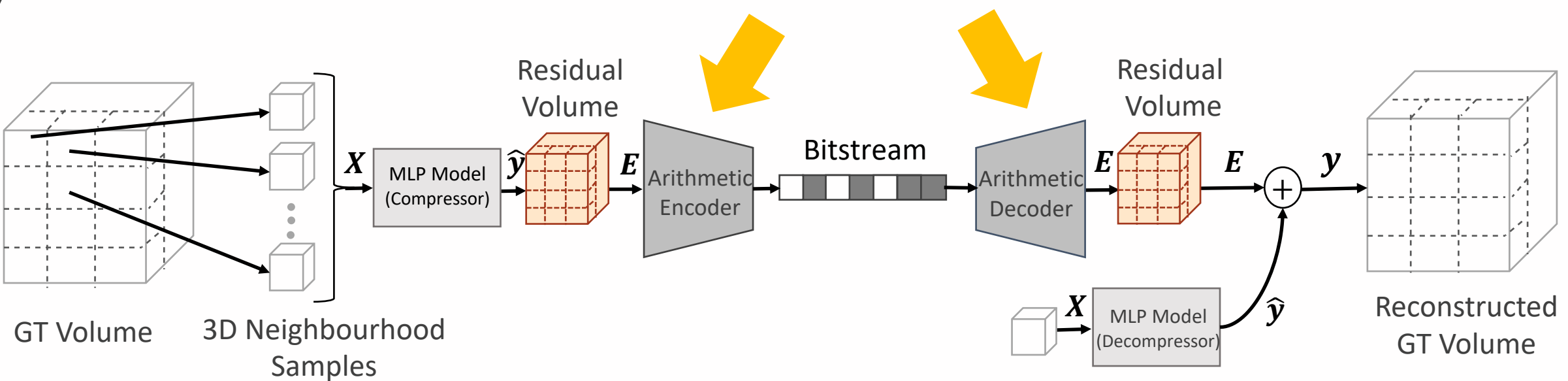
Proposed Method



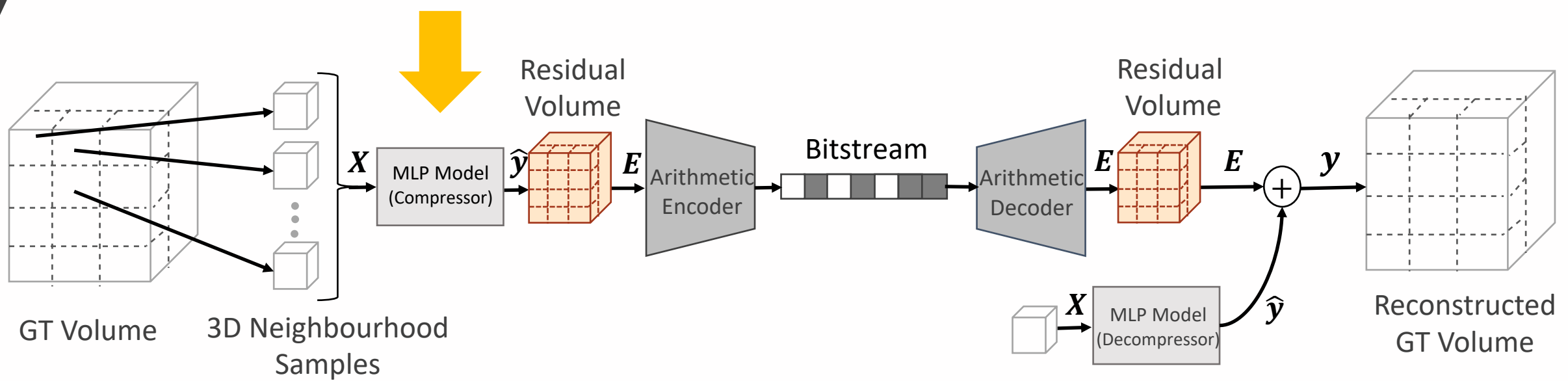
Proposed Method



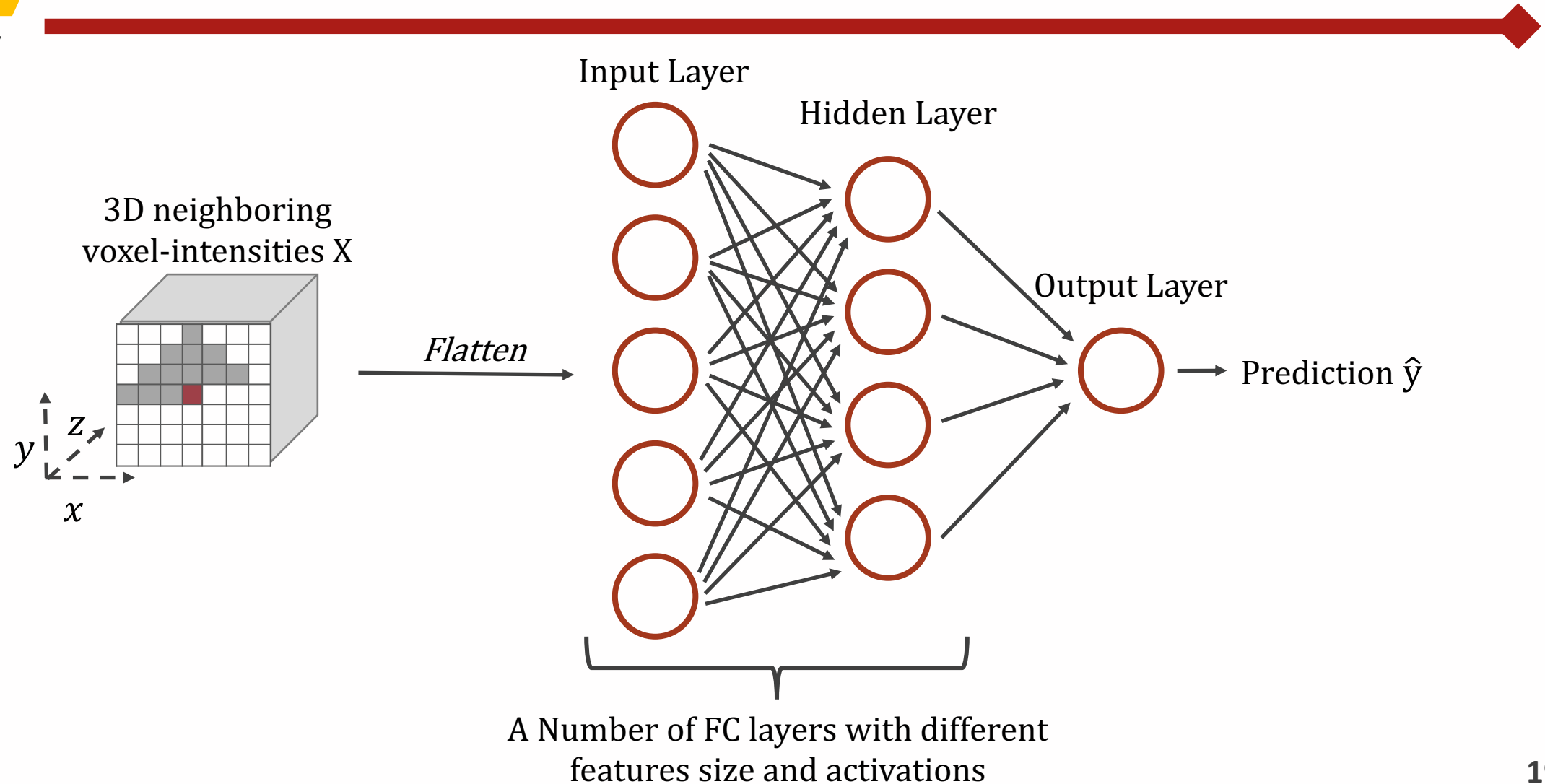
Proposed Method



Proposed Method



Network Architecture



Network Architecture

Layer	Number of Neurons	Activation Function Used
Fully Connected	1024	LeakyReLU
Fully Connected	512	LeakyReLU
Fully Connected	256	LeakyReLU
Fully Connected	128	LeakyReLU
Output	1	Linear

Local Sampling

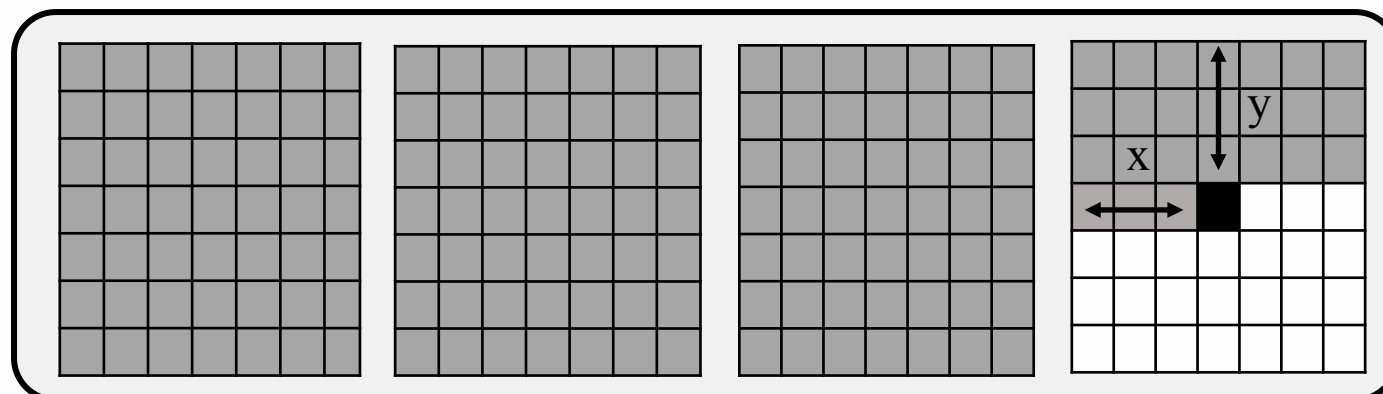
3D Cube
Neighboring
Sequence

$z = -3$

$z = -2$

$z = -1$

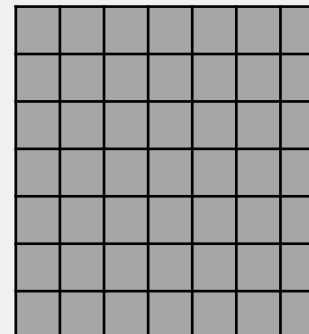
$z = 0$



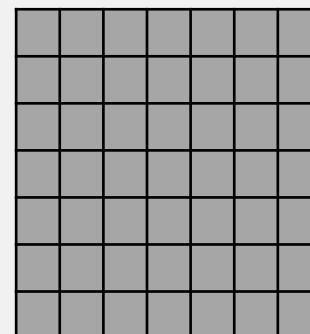
Local Sampling

3D Cube
Neighboring
Sequence

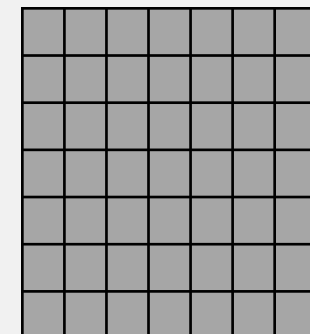
$z = -3$



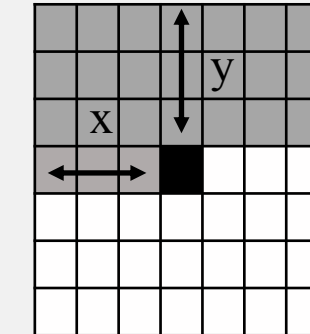
$z = -2$



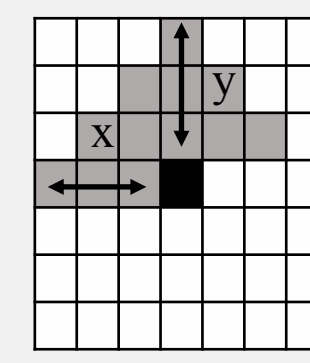
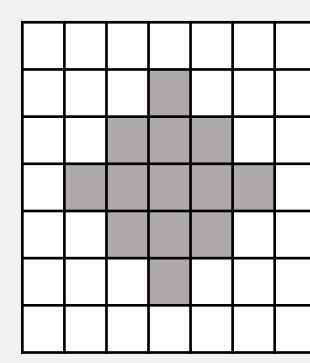
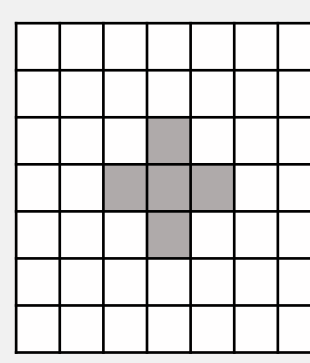
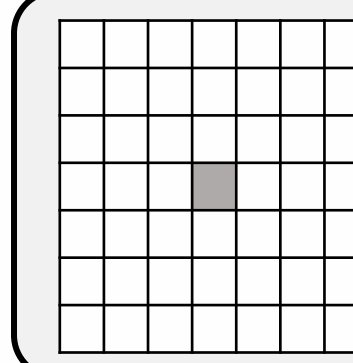
$z = -1$



$z = 0$



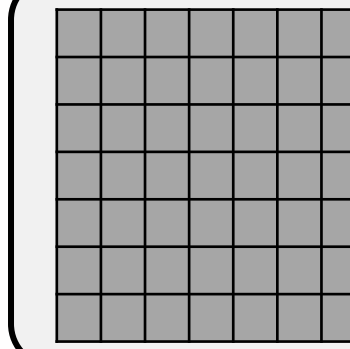
3D Pyramid
Neighboring
Sequence



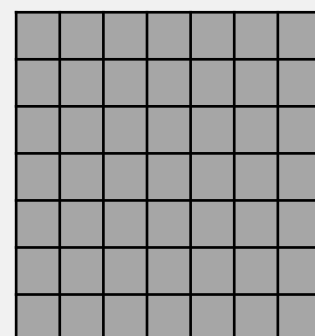
Local Sampling

3D Cube
Neighboring
Sequence

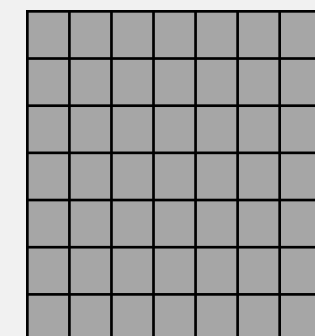
$z = -3$



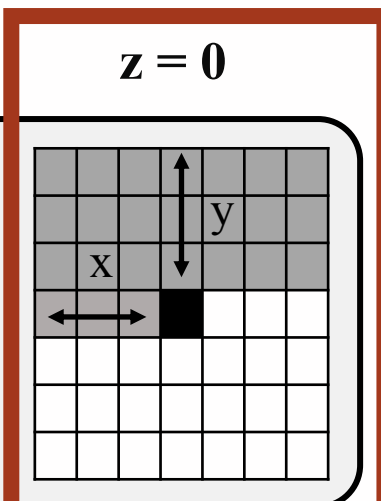
$z = -2$



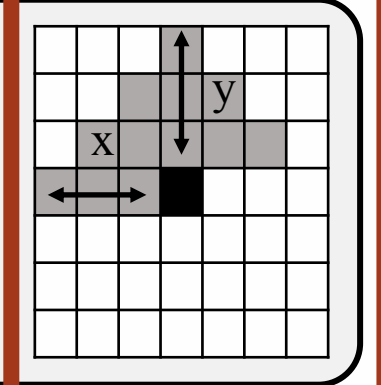
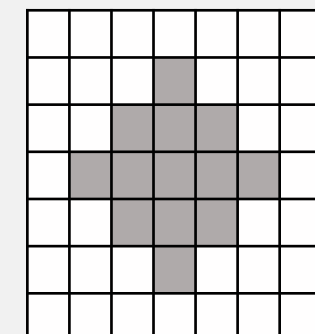
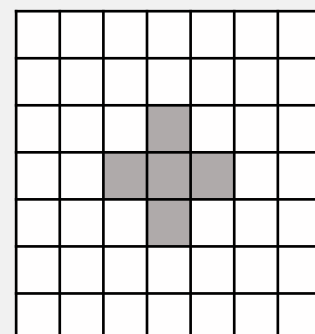
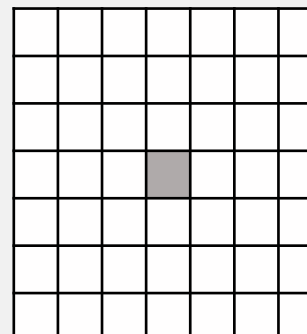
$z = -1$



$z = 0$



3D Pyramid
Neighboring
Sequence



Local Sampling

- ❖ All volume values are **normalized** to the range [-1,1] and the volume is padded, as **determined** by the block size, by its minimum voxel value.
- ❖ **Padding** the volume is crucial in order to include the **edge** and **corner cases** in training.
- ❖ All the **3D sequences** will be flattened to 1D vectors and **randomly shuffled** before inputting them to the **predictor models**.

Hyper Parameters

Model ID	Sampling Space	Shapes of the input Neighboring Block	Hyper Parameters
1	All samples were generated from 10 slices extracted from one volume (patient 40)	3D Cube input sequence (11x11x11)	Batch size = 256, learning rate = 2e-4, no L2 regularization, no dropout, and no batch normalization
2	All samples were generated from 10 slices extracted from one volume (patient 40)	3D pyramid input sequence (13x13, 9x9, 5x5, 1x1)	Batch size = 32, learning rate = 3e-5, no L2 regularization, no dropout, and no batch normalization

Loss Function

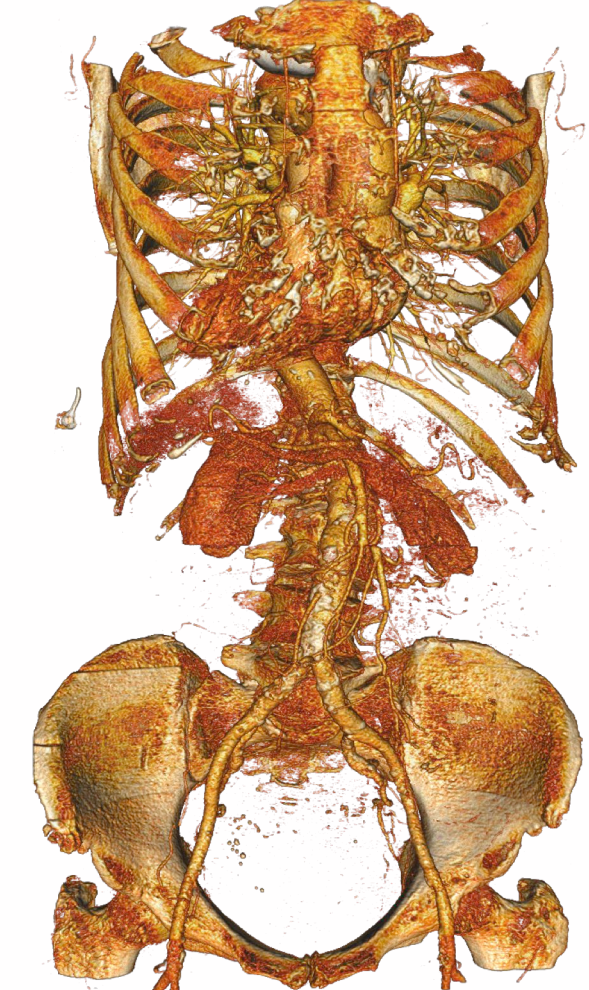
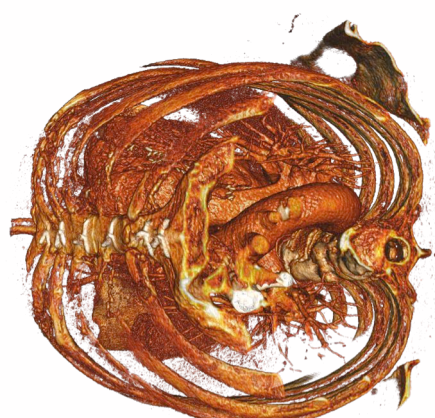
$$L_{Joint} = MAE + \lambda(1 - |PCC|)$$

$$MAE = \frac{\sum_{i=1}^n |y - \hat{y}|}{n}$$

$$PCC = \frac{cov(y, \hat{y})}{\sigma_y \sigma_{\hat{y}}}$$

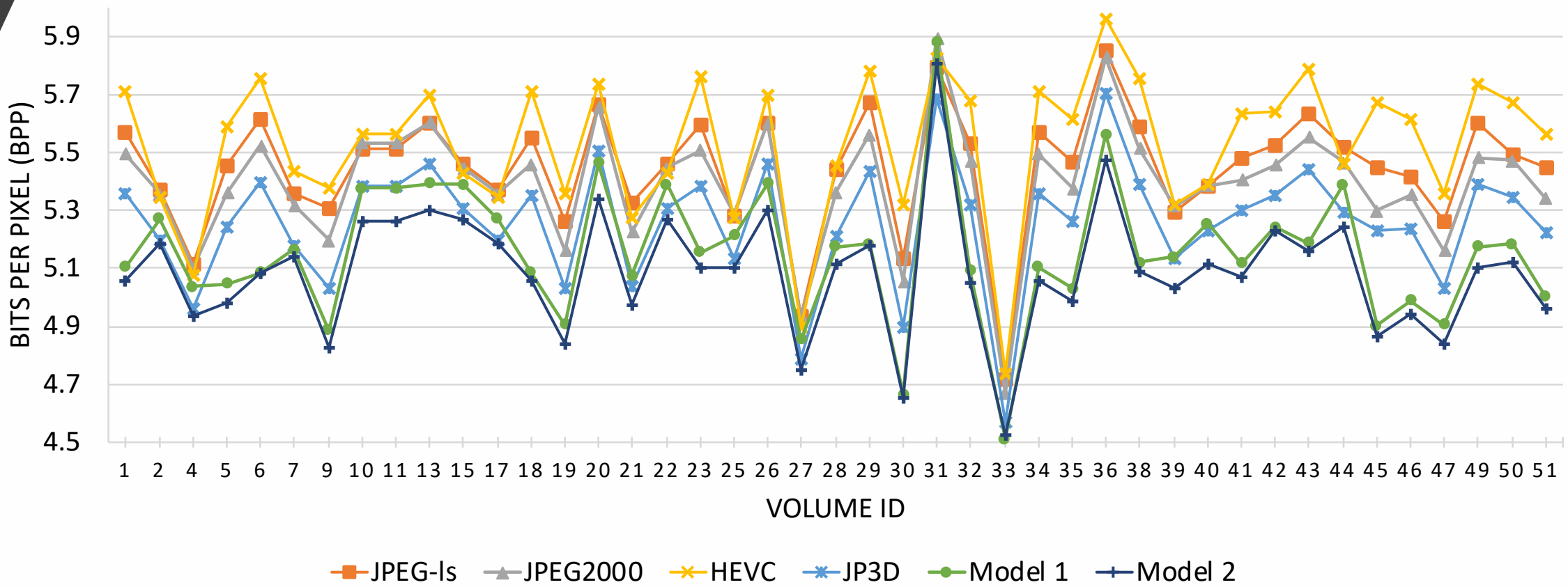
Result & Discussion

- ❖ We evaluated the **compression performance** in **bits-per-pixel (bpp)** of the proposed neural network models in comparison to the **state-of-the-art lossless compression** methods including JPEG-LS, JPEG2000, JP3D and HEVC.
- ❖ Our models were trained on one training set. However, the evaluation was conducted on two different test sets:
 - Testset1 (42 volumes)
 - Testset2 (2 volumes)



Result & Discussion (Testset1)

Comparing the compression ratio in BPP for the proposed models with the state-of-the-art lossless compression methods over 16-bits volumes on Testset1



Result & Discussion (Testset2)

Set Type	Volume ID	Pixel Spacing, Slice Thickness	JPEG-ls	JPEG2000	HEVC	JP3D	Model 1	Model 2
Training Set	40	0.625, 0.625, 0.625	5.387	5.387	5.389	5.23	5.256	5.119
Testset2 [18], [19]	CT Lung R004	0.830, 0.830, 5.00	5.937	6.014	5.739	5.967	6.664	6.715
	CT Lung R013	0.623, 0.623, 5.00	5.747	5.539	5.835	5.623	5.959	5.847

Result & Discussion (Testset2)

Set Type	Volume ID	Pixel Spacing, Slice Thickness	JPEG-ls	JPEG2000	HEVC	JP3D	Model 1	Model 2
Training Set	40	0.625, 0.625, 0.625	5.387	5.387	5.389	5.23	5.256	5.119
Testset2 [18], [19]	CT Lung R004	0.830, 0.830, 5.00	5.937	6.014	5.739	5.967	6.664	6.715
	CT Lung R013	0.623, 0.623, 5.00	5.747	5.539	5.835	5.623	5.959	5.847

Result & Discussion (Testset2)

Set Type	Volume ID	Pixel Spacing, Slice Thickness	JPEG-ls	JPEG2000	HEVC	JP3D	Model 1	Model 2
Training Set	40	0.625, 0.625, 0.625	5.387	5.387	5.389	5.23	5.256	5.119
Testset2 [18], [19]	CT Lung R004	0.830, 0.830, 5.00	5.937	6.014	5.739	5.967	6.664	6.715
	CT Lung R013	0.623, 0.623, 5.00	5.747	5.539	5.835	5.623	5.959	5.847
Resampled Testset2	CT Lung R004	0.625, 0.625, 0.625	5.459	5.243	-	5.195	4.915	4.904
	CT Lung R013	0.623, 0.623, 0.625	5.698	5.485	-	5.375	5.237	5.238

Conclusion

- ❖ We proposed a **novel lossless compression** system using a **neural network** for **volumetric** medical images (16 bit).
- ❖ Two **localized sampling** methods were introduced and evaluated on real **3D volumetric** medical imaging datasets.
- ❖ The comparison study shows that **our method outperforms** the standard lossless compression methods.
- ❖ It also suggests that the proposed method is **feasible** to generalize to unseen dataset while **retains satisfactory** performance.

Future Work

- ❖ Study of **generalization** across samples with different **pixel spacing** or **scan quality**.
- ❖ The effect of **model size** and **weight sparsity** on **compression ratio** from transmitting both the compressed representation and decoder.
- ❖ Optimization of the decoder to **leverage parallelism** over the **diagonal leading edge** to **reduce decode time**.

References

- 
- [1] David, T., & Marcellin, M. (2012). JPEG2000 Image Compression Fundamentals, Standards and Practice: Image Compression Fundamentals, Standards and Practice. Vol. 642.
 - [2] Weinberger, M. J., Seroussi, G., & Sapiro, G. (2000). The LOCO-I lossless image compression algorithm: Principles and standardization into JPEG-LS. *IEEE Transactions on Image processing*, 9(8), 1309-1324.
 - [3] Wu, X., & Memon, N. (1996, May). CALIC-a context based adaptive lossless image codec. In *1996 IEEE International Conference on Acoustics, Speech, and Signal Processing Conference Proceedings* (Vol. 4, pp. 1890-1893). IEEE.
 - [4] Matsuda, I., Mori, H., & Itoh, S. (2000, September). Lossless coding of still images using minimum-rate predictors. In *Proceedings 2000 International Conference on Image Processing (Cat. No. 00CH37101)* (Vol. 1, pp. 132-135). IEEE.
 - [5] Schelkens, P., Munteanu, A., Tzannes, A., & Brislawn, C. (2006, May). JPEG2000. Part 10. Volumetric data encoding. In *2006 IEEE International Symposium on Circuits and Systems* (pp. 4-pp). IEEE.
 - [6] Flynn, D., Marpe, D., Naccari, M., Nguyen, T., Rosewarne, C., Sharman, K., ... & Xu, J. (2015). Overview of the range extensions for the HEVC standard: Tools, profiles, and performance. *IEEE Transactions on Circuits and Systems for Video Technology*, 26(1), 4-19.
 - [7] Wu, X., & Memon, N. (2000). Context-based lossless interband compression-extending CALIC. *IEEE Transactions on Image Processing*, 9(6), 994-1001.
 - [8] Magli, E., Olmo, G., & Quacchio, E. (2004). Optimized onboard lossless and near-lossless compression of hyperspectral data using CALIC. *IEEE Geoscience and remote sensing letters*, 1(1), 21-25.
 - [9] Lucas, L. F., Rodrigues, N. M., da Silva Cruz, L. A., & de Faria, S. M. (2017). Lossless compression of medical images using 3-d predictors. *IEEE transactions on medical imaging*, 36(11), 2250-2260.

References

- 
- [10] Theis, L., Shi, W., Cunningham, A., & Huszár, F. (2017). Lossy image compression with compressive autoencoders. *arXiv preprint arXiv:1703.00395*.
 - [11] Lai, W. S., Huang, J. B., Ahuja, N., & Yang, M. H. (2017). Deep laplacian pyramid networks for fast and accurate super-resolution. In *Proceedings of the IEEE conference on computer vision and pattern recognition* (pp. 624-632).
 - [12] Toderici, G., Vincent, D., Johnston, N., Jin Hwang, S., Minnen, D., Shor, J., & Covell, M. (2017). Full resolution image compression with recurrent neural networks. In *Proceedings of the IEEE Conference on Computer Vision and Pattern Recognition* (pp. 5306-5314).
 - [13] Santurkar, S., Budden, D., & Shavit, N. (2018, June). Generative compression. In *2018 Picture Coding Symposium (PCS)* (pp. 258-262). IEEE.
 - [14] Ayoobkhan, M. U. A., Chikkannan, E., & Ramakrishnan, K. (2018). Feed-forward neural network-based predictive image coding for medical image compression. *Arabian Journal for Science and Engineering*, 43(8), 4239-4247.
 - [15] M. Goyal, K. Tatwawadi, S. Chandak and I. Ochoa. (2019). DeepZip: Lossless Data Compression Using Recurrent Neural Networks. In *2019 Data Compression Conference (DCC)*. (pp. 575-575). doi: 10.1109/DCC.2019.00087.
 - [16] Kingma, F. H., Abbeel, P., & Ho, J. (2019). Bit-swap: Recursive bits-back coding for lossless compression with hierarchical latent variables. In ICML.
 - [17] S. Dixon. (2018, Sep). Diagnostic imaging dataset statistical release. In NHS England, UK. Tech. Rep.
 - [18] B. Zhao, L. H Schwartz, and M. G Kris. (2015). Data fromrider lung ct. the cancer imaging archive. TCIA.
 - [19] Zhao, B., James, L. P., Moskowitz, C. S., Guo, P., Ginsberg, M. S., Lefkowitz, R. A., ... & Schwartz, L. H. (2009). Evaluating variability in tumor measurements from same-day repeat CT scans of patients with non-small cell lung cancer. *Radiology*, 252(1), 263-272.

The background of the image features two anatomical 3D renderings of a human body. On the left, a posterior view shows the spine, ribcage, and major organs in a reddish-brown color palette. On the right, a lateral view of the head and neck displays the brain, spinal cord, and surrounding structures. A large, semi-transparent white diamond shape overlaps both renderings, containing the text.

Thank you